Developing New Sustainable C-C Bond Forming Reactions

Joseph Phillipson

Supervised by Dr Russell Taylor

Department of Chemistry, Durham University

Abstract

Freidel-Crafts (FC) reactions have been a cornerstone of C-C bond formation in organic synthesis for decades. However, within the current drive for green chemistry, traditional FC reactions fall far short as result of their toxic reagents and catalysts. Alternative zeolite catalysis therefore provides an attractive alternative. This study finds evidence that the FAU zeolite approach for diaryl acetic acid synthesis, pioneered in the Taylor Group,[1] is suitable for bromobenzene and anisole. Further work is required for the characterisation of products in these cases, along with the selectivity of the processes. We also find that the procedure used is unsuitable for high boiling point naphthalenes, however we do not discount the approaches suitability for these compounds with an adapted procedure. Finally, we find that 2,5-dimethyl furan does not undergo the desired FC alkylation under these conditions, rather it will ring open into 3-hexene-2,5-dione as the major product.

Literature Perspective

Reactions that form C-C bonds have been the backbone of organic synthesis since its inception and continue to be the focus of extensive research.[1-3] Their applications span agriculture, pharmaceuticals, industrial chemical manufacturing and materials science,[3] highlighting the pressing need for green and sustainable approaches. Whilst many approaches exist and continue to emerge, Freidel-Crafts (FC) reactions have enjoyed widespread industrial and academic adoption.[4]

In 1877 Freidel and Crafts[5] accidentally performed the first Freidel-Crafts alkylation whilst attempting to study the effects of aluminium on amyl chlorides.[6,7] Since then Friedel-Crafts reactions have bloomed into the principal method for functionalisation of aromatics.[7] These reactions generally involve an electrophilic aromatic substitution between an electrophile and reactive nucleophile.[8] Classically, a homogenous strong Lewis or Brønsted acid catalyst is used,[7-10] $AlCl_3$ being the species used by Friedel and Crafts.[5] Their reaction first formed a carbocation or acylium ion, then proceeded through a Wheland intermediate to form the desired product through deprotonation (Fig.1).[6,11] However, subsequent approaches deviate from the classical carbocation or acylium ion generation.[11]

Unfortunatly, classical FC reactions do not meet the sustainable and green chemical standards of the 21st century, [12,13] principally because of the stoichiometric or superstoichiometric amounts of Lewis or Brønsted acid catalyst and alkyl halides required.[1,7-10,14,15] This results in vast amounts of salt side products, [7-9] thereby reducing the sustainability and profitability of the process. On top of this, the harsh conditions posed by the strong Lewis or Brønsted acid catalyst can results in poor functional group tolerance. This requires groups like amines to be protected, further reducing the atom economy and limiting its application for highly functionalised reagents.[14]

Scaling traditional FC reactions up to an industrial scale can be very hazardous when using alkyl halides, by virtue of their inherent toxicity,[1,7,9,10] corrosiveness[9,10] and environmental concerns. [4,16] This has led to regulatory incentives for their phasing out.[16] Super acids, like fluoroantimonic or triflic acid, can be used in place of the Lewis or Brønsted acid catalyst to accelerate the reaction[7] or when using deactivated substrates.[9,17] These too pose significant difficulties when applied to an industrial scale or even when handled in a lab. Super acids are extremely corrosive, hard to store and are a significant challenge to dispose of. Their extreme reactivity also yields poor functional tolerance, generally making them unattractive for fine and specialty chemical manufacturing.[18]

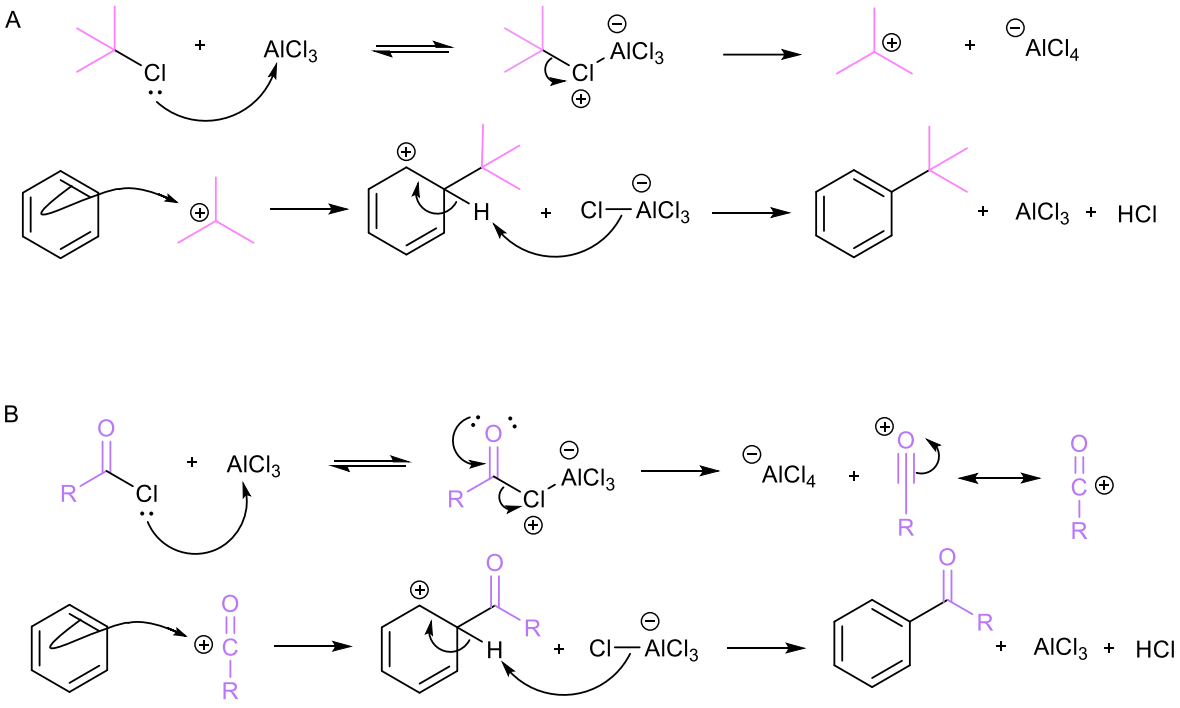

Figure 1. The reaction mechanism for a general Friedel-Crafts Alkylation (A) and Acylation (B) using an aluminium chloride catalyst

Many approaches have been developed to combat the problems highlighted above, with varying levels of success and adoption. π-activated alcohols have been a promising alternative for replacing classical alkyl halides, due to water being the only by-product produced. They consist of a hydroxy group adjacent to a π bonded system, which allows for easier activation of the C-OH bond via formation of stabilised cationic species.[4] Modern approaches are even able to perform a FC benzylation with a reactive heteroaromatic without the use of a Lewis acid catalyst and at 80°C.[7,19] Heterogenous catalysts have also proved effective in reducing catalyst waste through their ease of separation and superior reusability.[10,20] Furthermore, they display very high tunability[10,13,20] though variable pore sizes and selective doping, and a high selectivity,[20] making them extremely versatile. The scope of possible heterogenous catalysts for FC reactions is vast, encompassing metal-organic frameworks

(MOFs),[10,20] mesoporous superacid catalysts (MSCs),[10,15] clay (based) catalysts[10,13] and zeolites.[1,8,9] All have unique opportunities and suitability for different synthetic and industrial contexts, however from this point onwards, zeolites will be the focus.

There are currently 265 distinct zeolite frameworks that are known and are officially recognised.[21] The first natural zeolite was characterised by Axel Fredrik Cronstedt in 1756,[22] yet it was Richard Barrer's first successful synthesis of a zeolite in 1948[23] that has allowed them to bloom into one of the most diverse and widely applicable structural frameworks. Historically, zeolites were used by the Greeks and Romans as a cement additive and for water purification by the Mayans.[24] In the modern era, zeolites find use in industrial cracking,[22] carbon capture,[25] molecular sieves,[26] medicine[22] and many more – even in the cleanup of the Chernobyl nuclear disaster.[22,27]

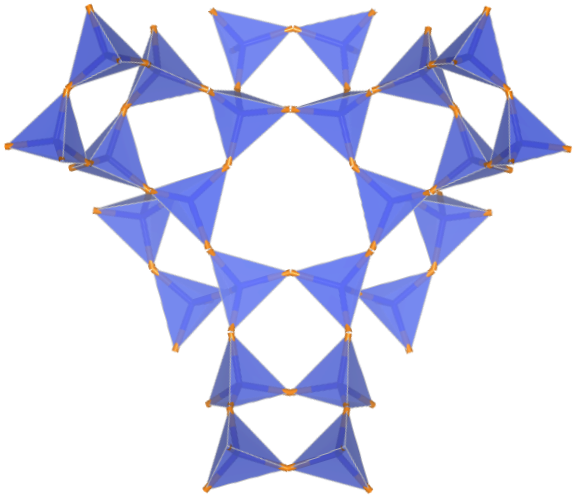

Figure 2. A section of the unit cell of the FAU zeolite displayed as polyhedra, with oxygen atoms being shown in pink and polyhedra in blue

Zeolites are crystalline microporous aluminosilicate materials composed of tetrahedral [SiO_4] and [AlO_4]$^-$ corner sharing units (Fig.2).[8,22] To maintain charge neutrality, these frameworks incorporate counterions, these normally being group 1 or 2 metal ions, or protons.[8] These protons are absolutely vital to the catalytic ability of the zeolite, as they form Si-(OH)-Al bridges that act as Brønsted acid sites (BAS) through their highly acidic proton (Fig.3).[28,29] The structure of the Lewis acid sites of a zeolite are less well defined. The net Lewis acidity of a zeolite is thought to be the agglomeration of the Lewis acidity of the framework aluminium, framework-associated aluminium and extra-framework aluminium, however this is out this works scope, so will not be explored further. Catalysis occurs as a result of the BAS; therefore, a range of catalytic properties can be achieved through tuning the abundance of such sites. The concentration of BAS can be changed by altering the Si/Al ratio as

the introduction of more or less $[AlO^4]^-$ will change the charge of the framework which will require a different number of counter ions to balance. However, there are limitations to the Si/Al ratio; zeolites, for the most part, obey Löwenstein's avoidance rule. This forbids the formation of Al-O-Al linkages because of the great coulombic repulsion between adjacent aluminium ions, hence imposing a lower limit on the Si/Al ratio. [8,30]

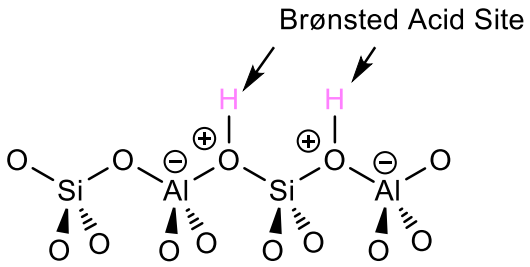

Figure 3. The Brønsted acid sites of a zeolite

Alongside their Brønsted acidity, the catalytic properties of zeolites can be further tuned through their porosity. All zeolites exhibit extensive microporosity (Fig.4), each micropore being characterised by a diameter of less than 2.0 nm.[26] These pore form networks of channels through which mass transport of reagents can occur and it is within these micropores that the catalyst's active sites are located.[31] They provide unique catalytic conditions, such as a huge surface area to volume ratio, nesting effects, confinement effects and crucially, shape selectivity. Nest effects are the tendency for the optimisation of the van der Waals interactions between the host pore and the guest molecule, resulting in an increase in the sorption equilibrium constant of said guest molecule. For this reason, molecules will nest in pores whose shape, size and length best optimise these van der Waals interactions, leading to an increase in local concentration of reagent and rate of reaction.[32] As this effect drives the selectivity and activity of the catalyst, the size of reagent molecules relative to pore size is vital when considering the compatibility of the catalyst. Closely related to nesting, is the shape selectivity and size exclusion of a zeolite. For a zeolite to effectively catalyse a reaction, the reactants must be able to reach the active site, the transition state must then be sterically small enough to fit within it and then finally the product must fit within the channels to leave the zeolite, otherwise the active sites will be become blocked.[26] A zeolite's ability to discriminate based on these factors enables then to direct reaction pathways in the desired direction and avoid side reactions[26] in a way that traditional homogenous catalysts are unable to achieve. Finally, confinement effects lead zeolites to act as solid solvent in their internal environment. This is a result of the aluminium and counter cation distribution generating electric field gradients unique to specific pore types. This is invaluable for catalysis as guest molecules can be polarised and have specific bond enthalpies reduced.[32]

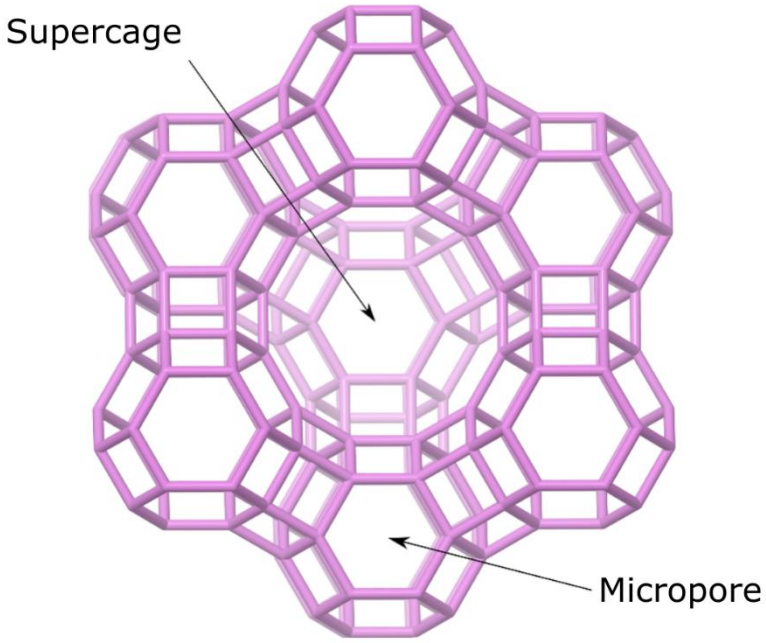

Figure 4. The framework of the unit cell of the FAU zeolite, with micropores and a supercage highlighted[22]

Micropores are key to the great versatility of zeolites, however their size can lead to a range of mass transfer limitations.[31,33] In zeolites, the main mechanism for mass transfer is diffusion, so if the rate of diffusion of the reactant molecules to the active site is slower than the rate of reaction, then the rate will be limited by mass transfer.[8] This problem is exacerbated by larger reagents, like aromatics, that may be larger than the pore diameter. Mass transfer limitation can be internal or external, where internal mass transfer limitations (IMTL) involve the movement of reactants through the zeolites internal pore/channel structure and external mass transfer limitations involve the rate of adsorption and desorption processes.[8] The result of such limitations are reduced catalytic activity, coking of the pores and side reactions before the reagents can reach the active site.[31] Hierarchical zeolites provide an elegant solution to these mass transfer limitation through the introduction of mesopores alongside micropores (Fig.4,5). Mesopores have a diameter greater than 2 nm and less than 50 nm, and provide excellent transport to internal sites, overcoming most IMTL and increasing the catalyst lifetime. Larger molecules will often only be able to enter the internal pore network of a hierarchical zeolite, the FAU zeolite used in this study is, itself a hierarchical zeolite. This allows it to accommodate the aromatic and polyaromatic nucleophile implicit in a FC alkylation, along with the equally bulky mandelic acid.

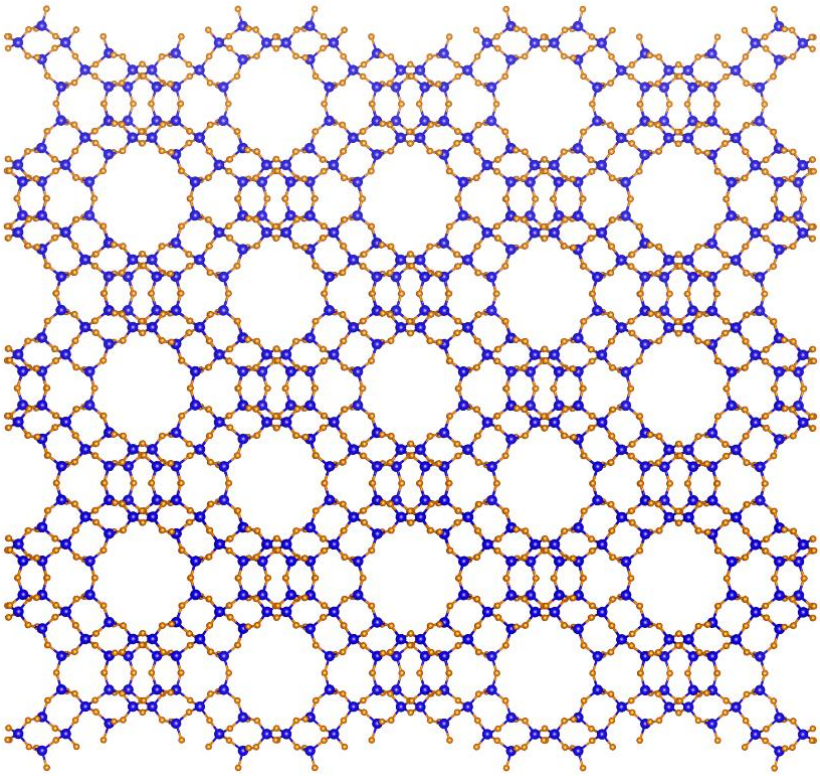

Figure 5. A portion of the FAU zeolite used to illustrate its mesoporous framework

Experimental

All reagents were purchased from Merck. Mandelic acid (0.200g, 0.00131 mol) was dissolved in an excess of the aromatic reagent (20cm^3 for boiling points less than 200°C and 0.8cm^3 for those over 200°C) and H-Y-30 zeolite (0.08g) was added. A phase separator was fitted to remove any water produced. The mixture was then allowed to reflux overnight for between 20 and 24 hours with stirring at 500 rpm throughout. Once refluxed, the mixture was filtered, the volatile components removed by rotary evaporation and a sample of the resulting solid/oil was dissolved in deuterated chloroform (0.5 cm^3; 6 mmol). ^{1}H and ^{13}C NMR was then performed on the product and NMR spectra recorded.

Results

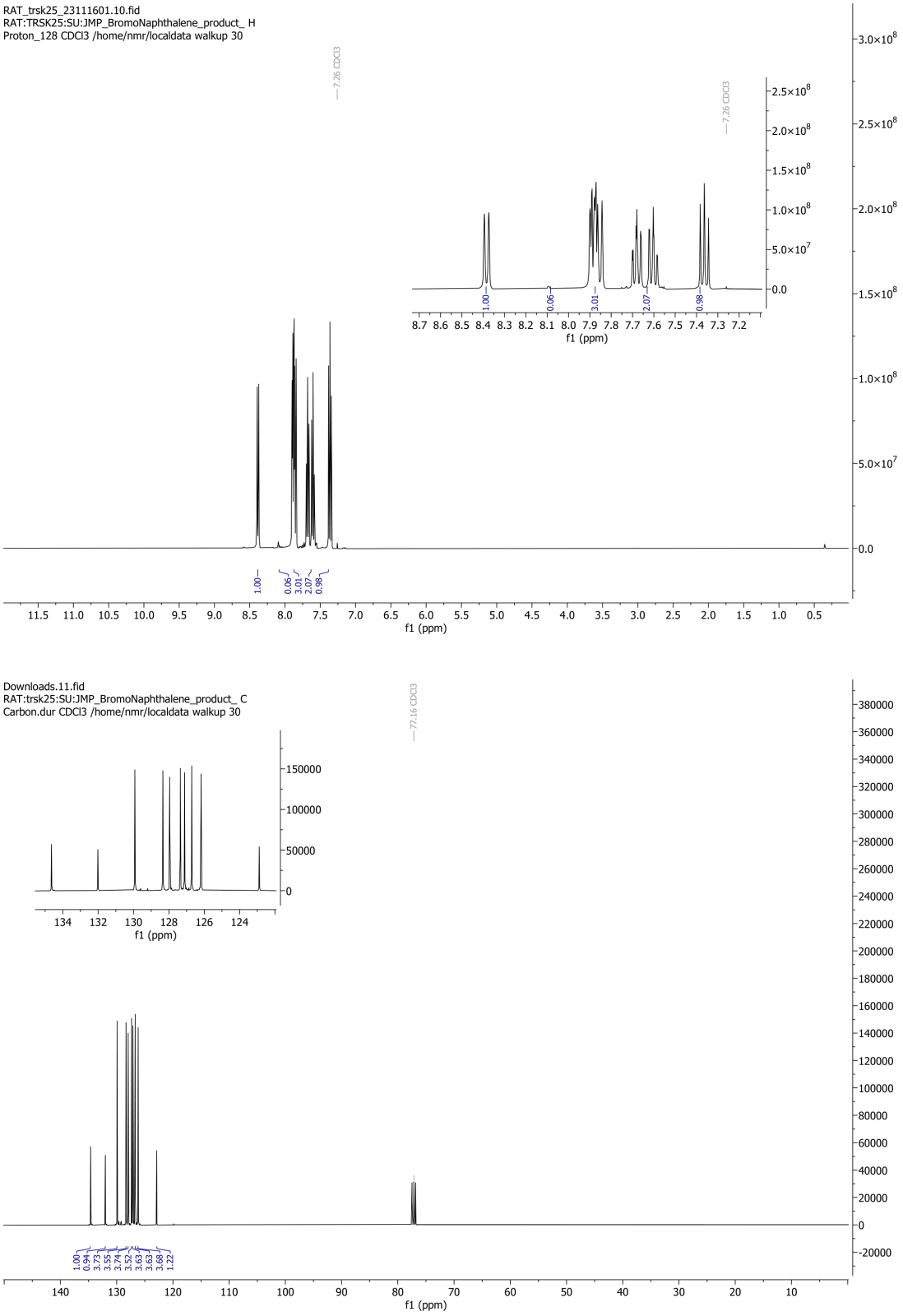

Figure 6. ^{1}H and ^{13}C NMR Spectrum (400MHz, $CDCl_3$) of the Product of the Reaction of 1-Bromonaphthalene and Mandelic acid, catalysed by the H-Y-30 Zeolite

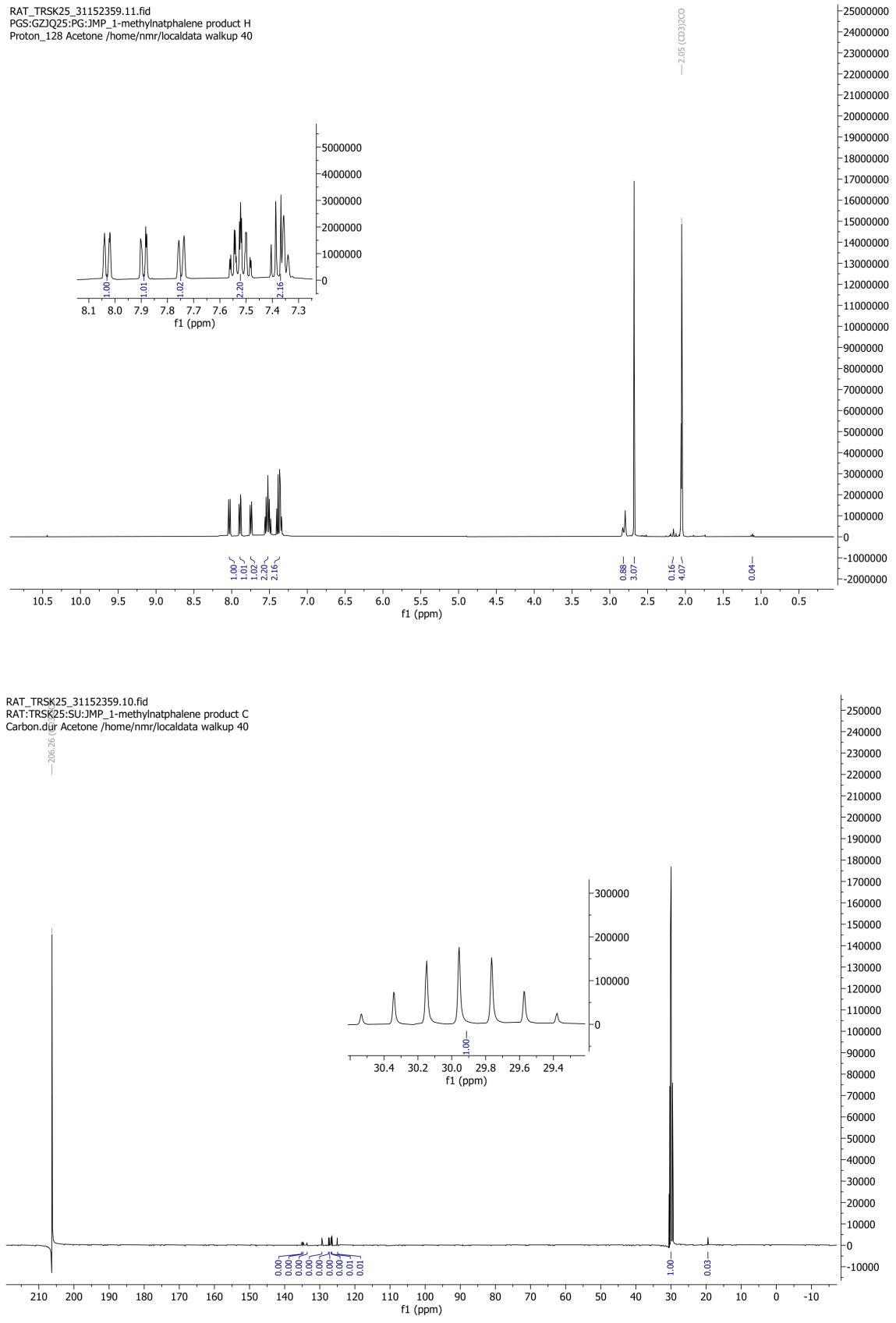

Figure 7. ^{1}H and ^{13}C NMR Spectrum (400MHz, Acetone-D6) of the Product of the Reaction of 1-Methylnaphthalene and Mandelic acid, catalysed by the H-Y-30 Zeolite

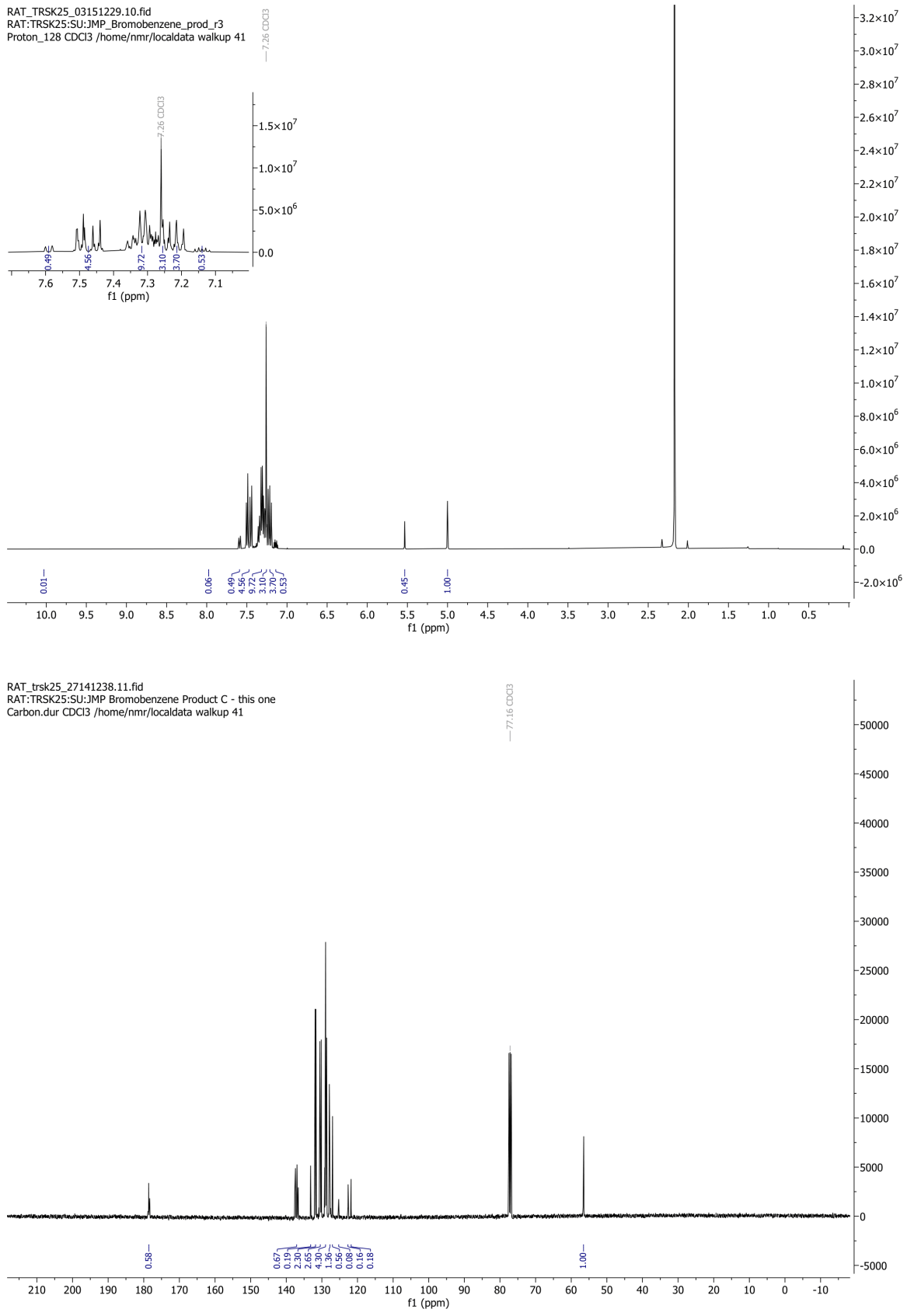

Figure 8. ^{1}H and ^{13}C NMR Spectrum (400MHz, $CDCl^{3}$) of the Product of the Reaction of 1-Bromobenzene and Mandelic acid, catalysed by the H-Y-30 Zeolite

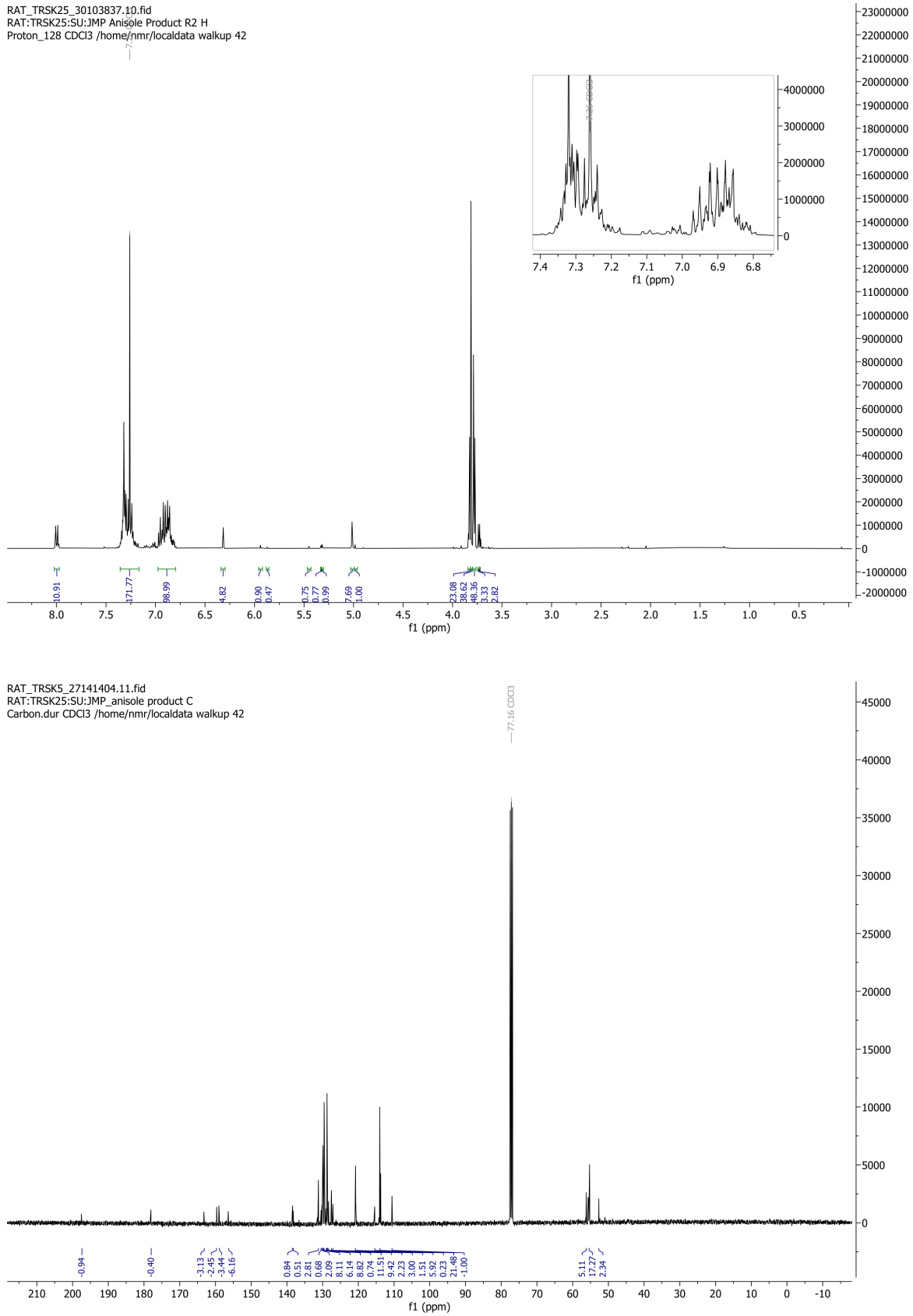

Figure 9. ^{1}H and ^{13}C NMR Spectrum (400MHz, $CDCl^{3}$) of the Product of the Reaction of Anisole and Mandelic acid, catalysed by the H-Y-30 Zeolite

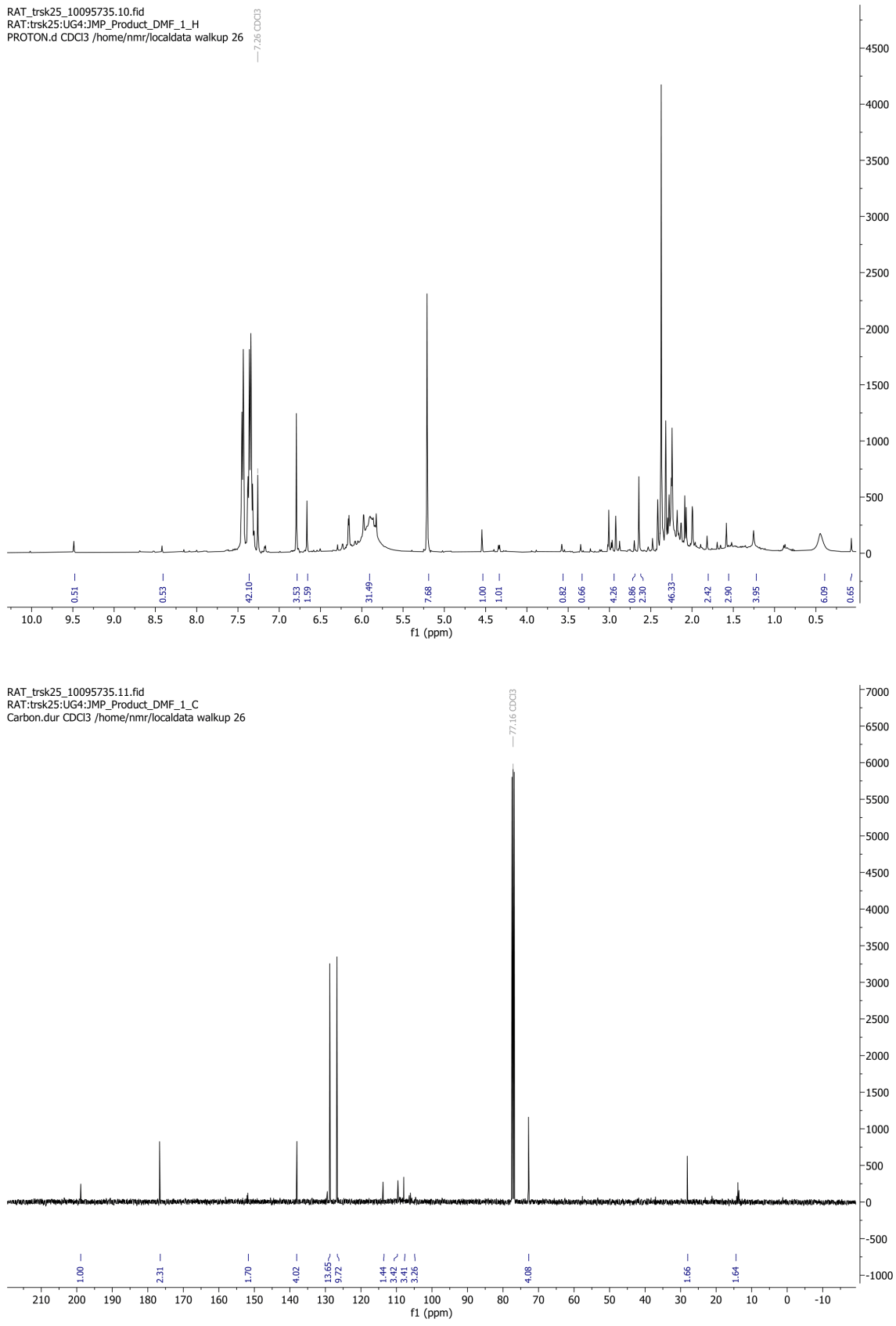

Figure 10. ^{1}H and ^{13}C NMR Spectrum (400MHz, $CDCl^{3}$) of the Product of the Reaction of 2,5-dimethyl furan and Mandelic acid, catalysed by the H-Y-30 Zeolite

Discussion

Large amounts of residual bromobenzene remain within the product, which is to be expected as the solvent was removed by a benchtop rotary evaporator, rather than in high *vacuo*. This is because of the high boiling point of bromobenzene (bp. 156°C).[34] The absence of peaks characteristic to mandelic acid suggest that it has fully reacted: δ_H (400MHz; $CDCl_3$) 4.68 (1H, s, OH) 5.24 (1H, s, CH). This is unsurprising, as the bromobenzene was in a 140:1 excess. In the previous work by Meacham *et al*[1] mandelic acid has been converted into a series of byproducts with varying selectivity (Fig 9.). No peaks are present that correspond to 2,5-diphenyl-1,3-dioxolan-4-one, the dimer or mandelide. No literature spectra were found for the latter two, so predictive spectra were used instead. A trace amount of benzaldehyde was observed in the ^1H spectra (Fig. 8): δ_H (400MHz; $CDCl_3$) 7.97 (5H, m) 10.02 (1H, s), which is in agreement with the literature.[35] The corresponding peaks are not visible in the carbon spectrum, however due to the poorer magnetogyric ratio and abundance of the ^{13}C isotope, the very low intensity benzaldehyde peaks could easily be lost in the noise. Repetition using a higher field NMR and a greater number of scans could confirm this. Peaks that are characteristic of the diarylacetic acid product are observed, particularly that which corresponds to the CH stereocentre (Fig. 8): δ_H (400MHz; $CDCl_3$) 5.00 (1H, s, CH), 5.54 (1H, s, CH). The presence of two peaks in this region suggests the presence of two isomers in a ~2:1 ratio. Whilst no literature spectra can be found to confirm the presence of these isomers, in the absence of any sizeable quantities of mandelic acid byproducts, these are likely the products.

The ^{13}C NMR spectra for the reaction of anisole with mandelic acid reveals the formation of a mixture of diaryl acetic acid isomers. Comparison with spectrum acquired by Kahn *et al.*[36] confirms the presence of the ortho and para isomers through characteristic ^{13}C chemical shifts: δ_C (400MHz; $CDCl_3$) 52.4, 55.0, 55.9, 110.5, 113.2, 120.6, 138.1, 138.3, 156.3, 159.6, 178.0. In the ^1H spectrum characteristic methoxy and methyl peaks are found in a 3:1 ratio: δ_H (400MHz; $CDCl_3$) 3.73 (3H, s, OCH_3), 3.74 (3H, s, OCH_3), 4.98 (1H, s, CH), 5.32(1H, s, CH). The spectrum holds further complexity in the methoxy, methyl and aromatic regions, suggesting the presence of the meta isomer, although no literature spectra can be found to confirm this. There was no formation of 2,5-diphenyl-1,3-dioxolan-4-one or benzaldehyde, which is confirmed through comparison to data from Meacham *et al*[1]. No literature spectra can be found for the dimer or mandelide, however predictive spectra do not suggest that these were produced. It is unlikely that residual mandelic acid accounts for any of these peaks because of the absence of mandelic acid peaks in the aromatic region. Acetone is observed in the product spectrum, likely because of insufficiently dried glassware: δ_H (400MHz; $CDCl_3$) 3.81 (6H, s). The anisole solvent was not fully removed from the product, so further purification would simplify the aromatic region. To fully identify all species present in the product, further purification and separation would be necessary. Performing the reaction in a stoichiometric ratio, rather than the

existing 140:1 excess might be useless as it would increase the concentration of product. The current procedure has the unwanted effect of concentrating any impurities present in the anisole into the product, therefore increasing the concentration of product would allow product peaks to be more easily identified. 2D NMR would be useful in determining the meta product peak in the cluttered methoxy region.

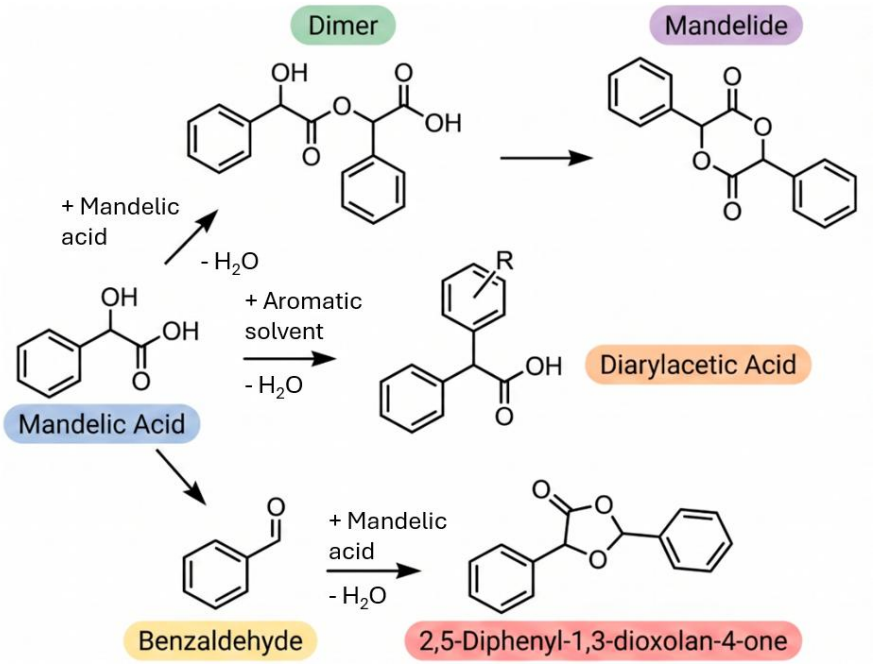

Figure 11. The possible byproducts of the reaction between Mandelic acid and an Aromatic solvent, adapted from Meacham *et al*[1]

The methodology used for both 1-bromonaphthalene and 1-methylnatphalenes was limited. Firstly, the oil bath used to heat the reactions was unable to reach the reflux temperature. 1-methylnapthalene (bp. 245°C)[37] reached 217 °C and 1-bromonaphalene (bp. 281°C)[38] reached 215°C, resulting in a lower conversion to product. Following this, the solvent was unable to be removed. Boiling at a high vacuum allowed the solution to reflux, with solvent condensing in the tubing connected to the flask. We were unable to prevent this as when the tube was insulated it melted. This resulted in product being dissolved in the excess of solvent. The NMR collected reflect this. In both the 1-bromo and 1-methylnaphthalene spectrum we see a large amount of unreacted solvent along with very low intensity peaks in the area indicative of product. These peaks are slightly higher in relative intensity in the 1-methyl naphthalene spectrum, reflecting the lower boiling point and resulting higher rate of reaction. It is undeniable that there has been some conversion of the reagents, however this methodology is insufficient to identify what they are or come to any solid conclusions.

Unexpectedly, the major product of the reaction of 2,5-dimethylfuran (DMF) and mandelic acid was 3-hexene-2,5-dione (DAE): δ_C (400MHz; $CDCl_3$) 28.10, 138.03, 198.85. This was verified by comparison to the ^{13}C spectrum acquired by Christensen *et al*.[39] They propose a hydroxy and hydroperoxy radical ring opening mechanism (Fig. 12); however, a thermodynamics study would be required to verify if the same mechanism is at play here. A large variety of other products are observed in the complex ^1H NMR spectrum. This is most likely a complex mixture of oligomers formed from the reaction of polar ring opening products and starting DMF reported by Christensen *et al*.[39] They found the that 50% of product was DAE, which seems qualitatively similar to the product distribution of this study, although quantitative NMR would be required to verify this. Further separation through column chromatography would be informative about the makeup of the minor products. Miedziak *et al.*[40] report that DAE is able to ring close to furaneol with a gold catalyst, however this is not observed under these conditions. Mandelic acid appears unreacted in the product spectrum: δ_C (400MHz; $CDCl_3$) 72.80, 126.76, 128.72, 128.76, 138.13, 176.68. DMF does not appear in the product spectra, likely as a result of its lower boiling point (bp. 94°C)[41] leading to a higher conversion and more complete removal of excess solvent by rotary evaporation. Overall, this suggests that the mandelic acid and the DMF did not react together, rather the DMF underwent a ring opening and subsequent oxidation within the zeolite, independent of the mandelic acid.

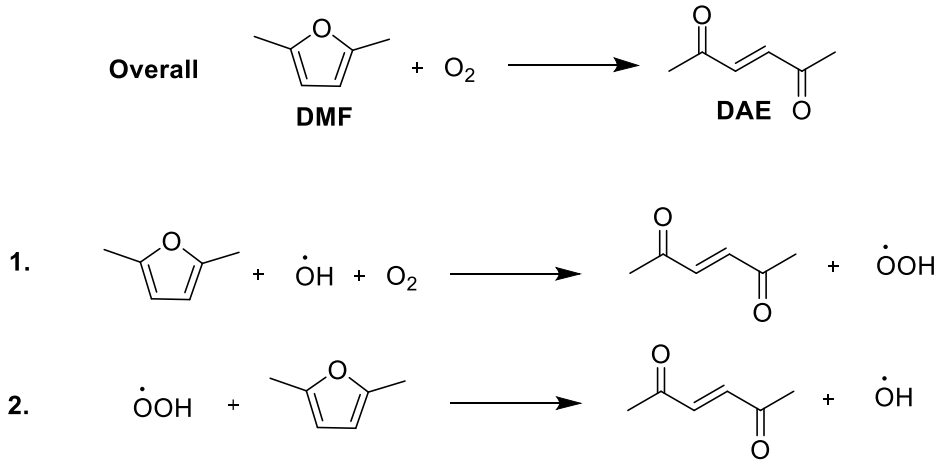

Figure 12. The overall reaction for the formation of DAE from DMF outside of a zeolite. (1,2) The individual radical mechanism steps proposed by Christensen *et al*.[38]

Conclusion

The procedure used was found to be suitable for only the lower boiling point monoaromatic reagents, being limited by heating ability of the equipment and difficulty in removing the solvent. For those where the procedure was suitable, anisole and bromobenzene produced the desired diarylacetic acid. Each produced a mixture of the possible isomers with further work being required to identify the product selectivity and isolate the products. The current procedure also concentrated any impurities present in the reagents and therefore further runs at closer to stoichiometric ratios would be beneficial in identifying impurities. Finally, 2,5-dimethyl furan underwent a ring opening mechanism to produce 3-hexene-2,5-dione and did not react with the mandelic acid. Therefore, we concluded that under these conditions, the FAU zeolite approach is unsuitable for DMF.

References:

1. S. G. Meacham, R. A. Taylor, Chem. Commun., 2023, **59**, 9243
2. A. Sikder, J. Sengupta, Org. Biomol. Chem., 2025, **23**, 2539
3. X. Guo, Z. Bai, Z. He, Y. Tian, S. Zhan, Sci. China Chem., 2026, **69**, 1580
4. C. Friedel, J.M. Crafts, Compt. Rend., 1877, **84**, 1392
5. C. Goedecke, Charles Friedel and the Accidental Discovery of an Important Reaction, https://www.chemistryviews.org/charles-friedel-and-the-accidental-discovery-of-an-important-reaction/ [Accessed: 27/07/2026]
6. M. Rueping, B. J. Nachtsheim, Beilstein J. Org. Chem., 2010, **6**, 1
7. E. F. Garland, Mchem Dissertation, Durham University. 2024
8. M. L. Gault, Mchem Dissertation, Durham University 2023
9. J. Ohata, Org. Biomol. Chem., 2024, **22**, 3544
10. A Comparative Yield Analysis: Friedel-Crafts Acylation vs. Suzuki Coupling for the Synthesis of 2-Aminobenzophenones, Bench Chem., 2026
11. J. Starvaggi, R. Ettari, Multi. Digi. Pub. Instit., 2025,**18**, 1692
12. M. Bandini, M. Tragni, J. Org. Biomol. Chem., 2009, **8**, 1501
13. K. Sachidanandan, A. Umunnah, A. Hahn, S. Laulhe, RSC Adv., 2025, **15**, 43155
14. S. Fukuzawa, T. Tsuchimoto, T. Hiyama, J. Org. Chem. 1997, **62**, 151
15. Transformative Effects of Fluoroantimonic Acid in Chemistry, https://eureka.patsnap.com/report-transformative-effects-of-fluoroantimonic-acid-in-chemistry [Acessed: 27/07/2026]
16. P. Cozzi, L. Zoli, Angew. Chem., 2008, **47**, 4162
17. R. Singh, G. Singh, N. George, G, G. Singh, S. Gupta, H. Singh, G. Kaur, J. Singh, Catalysts, 2023, **13**, 130

18. L. T. L. Nguyen, C. V. Nguyen, G. H. Dang, K. K. A. Le, N. T. S. Phan, Mol. Catal., 2011, **349**, 28
19. G. Yadav, G. George, Micro. Meso. Materials, 2006, **96**, 36
20. S. Dasgupta, B. Török, Org. Prep. Proced. Int.., 2008, **40**, 1
21. Database of Zeolite Structures, IZA Structure Commission, https://www.iza-structure.org/databases/ [Accessed 30/07/2026]
22. A. M. Alotaibi, Molecules, 2025, **30**, 4036
23. R. M. Barrer, J Chem Soc., 1948, 127
24. K. Tankersley, N. Dunning, C Carr, D. Lentz, V. Scarborough, Sci. Rep., 2020, **10**, 18021
25. K. Sumida, D. Rogow, J. Mason, T. McDonald, E. Bloch, Z. herm, T. Bae, J. Long, Chem. Rev. 2012, **112**, 724
26. A Corma, Chem. Rev., 1997, **97**, 2375
27. Nuclear Remediation with Zeolite, ISA Ore Zeolite, https://ida-ore.com/uses-for-zeolite/nuclear-remediation-with-zeolite/ [Accessed 30/07/2026]
28. M. Trachta, O. Bludsky, J. Vaculik, R. Bulanek, M. Rubes, Sci. Rep., 2023, **13**, 12380
29. M. Ravi, V. Sushkevich, J. Bokhoven, Nat. Mater., 2020, **19**, 1047
30. R. Fletcher, S. Ling, B. Slater, Chem. Sci., 2017, **8**, 7483
31. L. Chen, M. Sun, W. Yang, Z. Xie, B. Su, Chem. Rev., 2020, **120**, 11194
32. G. Sastre, A. Corma, J. Mol. Catal. A, 2009, **305**, 3
33. N. Hijazi, A. Bavykina, I. Yarulina, T. Shoinkhorova, E. Ramos-Fernandez, J. Gascon, Chem. Soc. Rev., 2025, **54**, 6335
34. Merck, Merck, https://www.sigmaaldrich.com/GB/en/product/aladdinscientific/alnh9a9f536a [Accessed 02/09/2026]
35. Chemical Book, https://www.chemicalbook.com/SpectrumEN_100-52-7_1HNMR.htm [Accessed 06/08/2026]
36. J. Kahn, A. Tyagi, R. Samanta, C. K. Hazra, Chem. Commun., 2024, **60**, 10688
37. Ficher Scientific, https://www.fishersci.co.uk/shop/products/1-bromonaphthalene-97-thermo-scientific/11498086 [Accessed 17/08/26]
38. Merck, https://www.sigmaaldrich.com/GB/en/product/aladdinscientific/alnh9a9f536a [Accessed 17/08/26]
39. E. Christensen, G. M. Fioroni, S. Kim, L. Fouts, E. Gjersing, R. S. Paton, R. L. McCormick, Fuel, 2018, **212**, 576
40. P. J. Miedziak, J. K. Edwards, S. H. Taylor, D. W. Knight, B. Tarbit, G. J. Hutchings, Catal. Lett., 2018, **148**, 2109
41. Merck, https://www.sigmaaldrich.com/GB/en/product/aldrich/177717?srsltid=AfmBOorMnIbGCPEf LluU6M3qfOa-eKrNv1N149VUCXPz6i1MYac_VIS8 [Accessed 19/08/26]